Zhao, G.-Y. et al., 2018, *AJ*, **155**, 26

4. Explosive phenomena, transients

Transient sources of electromagnetic radiation are ideal sites to probe extreme physics. Some of the transient source classes provide the most luminous objects in the Universe, for the duration of the outburst. In the radio regime we distinguish between two broad types: broad-band, incoherent transient sources of non-thermal (typically synchrotron) radiation with a duration much longer than a few seconds, and coherent fast transients that last shorter than 2s.

Since transients are initially very compact, and can be very bright, they are natural targets for very high resolution observations. Arrays like the EVN, that consist of telescopes that are not fully dedicated to VLBI observations all year round, have had limited capabilities in addressing high impact transient science. This all changed with the development of the electronic VLBI technique, that allowed flexible organisation of regular, as well as Target of Opportunity e-EVN sessions (Szomoru 2008). The EVN transient science, and the first ten years of e-EVN work in particular is summarised by Paragi (2017). Below we describe the transient science the EVN could address in the future, for both incoherent (Sect. 1.) and coherent types (Sect. 2.) of transients.

4.1 Synchrotron transients

The first ever published science results using the e-EVN was observations of 'microquasars' Cyg X-1 (Rushton et al. 2007) and Cyg X-3 (Tudose et al. 2007). Therefore we start with radio-jet X-ray binaries, and describe other major transient classes in subsequent sections.

4.1.1 Black hole and neutron star X-ray binaries

Jets are now believed to be a common feature of accreting neutron star (NS) and black hole (BH) X-ray binaries (XRBs), with properties that depend on the nature of the accretion flow. Although they have only been directly resolved in the most luminous systems (e.g. Tingay et al. 1995, Spencer et al. 2013) their presence is often inferred through broadband spectra (typically including a spectral break between radio and infrared frequencies; e.g. Migliari et al. 2010), polarisation measurements

Chapter image: Jet breaking through the kilonova ejecta following the merger of two neutron stars. Beabudai Design.

indicating synchrotron emission (e.g. Corbel et al. 2000), or through their location and evolution in the radio/X-ray luminosity plane (e.g. Gallo et al. 2006).

While there are a handful of persistent radio-emitting XRBs, the majority of systems are transient. Outbursts of these transient systems show a large dynamic range in accretion rate, leading to significant changes in the geometry of the accretion flow and the morphology of the jets. These changes, typically occurring on timescales of days to weeks, allow us to study the universal coupling between accretion and ejection, which cannot be as easily probed in more slowly varying AGN.

The other key advantage of XRBs in studying jets is the range of accretor properties. Comparative studies of jets from BH and NS systems can elucidate the effect of the stellar surface and the depth of the gravitational potential well on the formation of jets. Furthermore, since magnetic field strengths and spin periods can be directly measured in NSs, we can readily explore their effect on jet formation. However, the relative radio faintness of NS XRBs has meant that to date they have been much less well studied with VLBI than their BH counterparts. Future VLBI sensitivity upgrades would therefore facilitate more detailed comparisons of jets from NS and BH systems.

High-resolution imaging

The past few decades of observational effort (primarily on the radio-brighter BH systems) have led to a paradigm in which the compact, steady radio jets that exist at low luminosities are quenched at the peak of an X-ray outburst, giving way to bright, relativistically-moving transient ejecta (e.g. Fender et al. 2004). Understanding how these jets are launched is one of the major open questions in the field. With time-resolved VLBI imaging, we can trace moving jet components back to the time of ejection, enabling us to pinpoint any X-ray spectral or variability signatures associated with the ejection event. This cannot be achieved using radio light curves alone, both due to optical depth effects and the difficulty of distinguishing direct jet emission from interactions with the surrounding medium (e.g. Rushton et al. 2017). While new methods of probing the jet base using high time resolution optical observations can provide complementary probes of the jet launching process, VLBI imaging allows a direct causal connection to be made between jet ejection events and the associated changes in the accretion flow. Future X-ray polarimeters (e.g. *IXPE* and *XIPE*) will also determine the inclination angle of the inner accretion flow. Together with jet proper motions from VLBI and optical constraints on the binary orbit, this will provide a powerful probe of the geometry of the system, including any warping or precession of the disk and their impact on the jets.

The rapid changes in both morphology and brightness on the timescale of a few-hour observation (as shown in Fig. 4.1) pose significant challenges for VLBI imaging of XRB jets. Splitting an observation into short time bins requires a source that is both sufficiently bright and structurally simple that its radio morphology can be reconstructed with minimal *uv*-coverage. Spurred by similar challenges for the Event Horizon Telescope, new algorithms are therefore being developed that will enable much-improved imaging of time-variable sources (e.g. Johnson et al. 2017).

One underexplored area that would benefit greatly from extra sensitivity is VLBI polarimetry of XRB jets. The lower resolution and lower surface brightness of XRB jets (as compared to AGN) has meant that the signal-to-noise ratio is not always sufficient to detect polarised emission, and most of our knowledge of the magnetic field structure in XRB jets stems from integrated radio flux densities from lower-resolution facilities such as ATCA or the VLA.

Another open question is how relativistic XRB jets can be. While a few cases of apparent superluminal motion have been observed (Mirabel et al. 1994; Tingay et al. 1995; Hjellming & Rupen 1995), the Lorentz factors of most XRB jets are very poorly constrained. However, it has been suggested that their Lorentz factors could reach $\Gamma > 10$, rivalling the jets of AGN (Miller-Jones

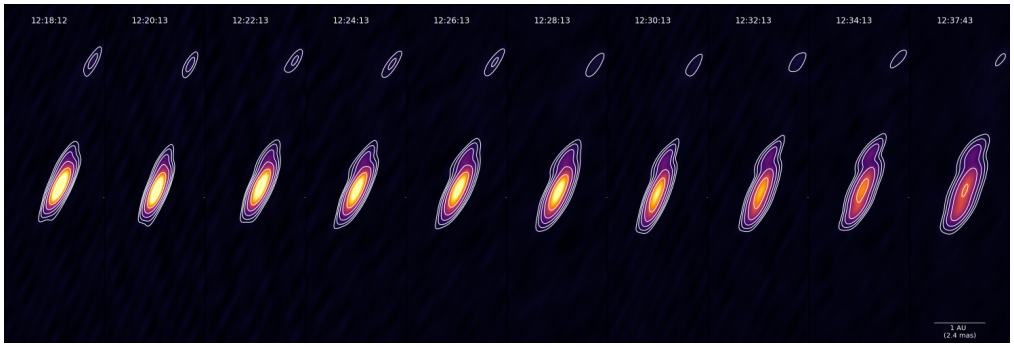

Figure 4.1: Time-resolved VLBA imaging of the BH XRB V404 Cyg on 22 June 2015 (time of each image shown in UT). The source evolves during each 2-minute snapshot (Miller-Jones et al. 2019).

et al. 2006). This question, which significantly affects the inferred energetics of the jets, can be answered by measuring the proper motions of corresponding approaching and receding jet ejecta in sources with accurate distances (Mirabel & Rodríguez 1999; Fender 2003).

Astrometry

As core-dominated radio sources, XRBs in their hard or quiescent states provide excellent astrometric probes, allowing parallax and proper motion measurements. Even with the advent of *Gaia* DR2, only eleven BH XRBs have optical parallax measurements, with only three being significant at $\geq 4\sigma$ (Gandhi et al. 2019), such that distance estimates rely heavily on the choice of prior. Since many XRBs lie towards the Galactic bulge, the visual extinction is often too high to detect an optical counterpart, and high-precision VLBI astrometry will continue to play an important role in this area. However, the majority of systems are too radio-faint to be detected in quiescence, so astrometric campaigns must be undertaken during irregular outbursts. The advent of synoptic optical surveys by facilities such as ZTF and LSST will enable earlier detection of new outbursts, allowing us to obtain better astrometric sampling during the rising quiescent and hard state phases.

While distance measurements require extremely high precision and appropriate sampling of the parallax ellipse, XRB proper motions are significantly easier to measure, since the signal is both larger (a few mas yr^{-1}) and cumulative. Together with an accurate distance and an optical or infrared measurement of the systemic radial velocity, XRB proper motions can be used to determine the full three-dimensional space velocity of the system. Modelling of the Galactocentric orbit together with the binary evolution of the system (e.g. Willems et al. 2005) can provide excellent constraints on the process in which the compact object formed – whether in a natal supernova, or (in the case of BHs) by direct collapse. In the case of a supernova, both the recoil and any asymmetries in the explosion can lead to significant natal kicks, the distribution of which is still poorly observationally constrained. The first detections of gravitational waves from merging BHs and NSs has given renewed importance to determining the kick distribution, since large kicks will both unbind a primordial binary in the field, or eject a compact object from a globular cluster before it has a chance to dynamically form a binary. Thus, stronger natal kicks should reduce the rate of merger events (Wysocki et al. 2018). While the strongest natal kicks should unbind the progenitor binary system, milder kicks can introduce eccentricity into a binary orbit, thereby increasing the probability of a merger (Giacobbo & Mapelli 2018). Hence the differing biases of gravitational wave observations and X-ray binary astrometry provide different insights into the compact object formation process.

Proper motions can also be used to discriminate Galactic objects from extragalactic background sources, for example in deep radio surveys of dense regions such as the Galactic bulge or the globular cluster population (e.g. Strader et al. 2012). While population synthesis codes (e.g. Yungelson et al. 2006) predict $\gtrsim 10^4$ BH XRBs within the Milky Way, only a few dozen candidates are known. The remainder of the population may be transients that have either been in quiescence since the dawn of X-ray astronomy, or whose outbursts are too faint to trigger all-sky monitors. However, their radio jets could be detected in quiescence, and distinguished from extragalactic background sources via their proper motions and parallaxes, as was done recently for a BH candidate toward M15 (Kirsten et al. 2014; Tetarenko et al. 2016). Sensitive, wide-field VLBI surveys could reveal a larger fraction of this population. Finally, it has been suggested that with sufficient sensitivity, astrometric observations could even detect nearby isolated BHs accreting from the ISM (Fender et al. 2013), thereby revealing some of the closest BHs to Earth.

With sufficiently high precision, astrometry can not only measure the parallax and proper motion of an XRB, but also (for wide binaries) measure the orbit of the compact object. For systems with sufficiently bright optical counterparts, the combination of optical astrometry from *Gaia* and VLBI astrometry in the radio band could measure the orbits of both donor and accretor, thereby enabling us to determine the full set of system parameters, including the masses of both components (e.g. Miller-Jones et al. 2018). Such geometrically-determined masses could provide some of the most robust, model-independent mass estimates available for NSs and BHs.

4.1.2 Thermonuclear runaway supernovae

Type Ia SNe are the end-products of white dwarfs (WDs) with a mass approaching, or equal to, the Chandrasekhar limit, which results in a thermonuclear explosion of the star. While it is well acknowledged that the exploding WD dies in close binary systems, it is still unclear whether the progenitor system is composed of a C+O white dwarf and a non-degenerate star (single-degenerate scenario), or both stars are WDs (double-degenerate scenario). In the single-degenerate scenario, a WD accretes mass from a hydrogen-rich companion star before reaching a mass close to the Chandrasekhar mass and going off as supernova, while in the double-degenerate scenario, two WDs merge, with the more-massive WD being thought to tidally disrupt and accrete the lower-mass WD (e.g., Maoz et al. 2013) This lack of knowledge makes it difficult to gain a physical understanding of the explosions, and to model their evolution, thus also compromising their use as distance indicators.

Radio and X-ray observations can potentially discriminate between the progenitor models of SNe Ia. For example, in all scenarios with mass transfer from a companion, a significant amount of circumstellar gas is expected (e.g. Branch et al. 1995), and therefore a shock is bound to form when the supernova ejecta are expelled. The situation would then be very similar to circumstellar interaction in core-collapse SNe (see above), where the interaction of the blast wave from the supernova with its circumstellar medium results in strong radio and X-ray emission (Chevalier 1982). On the other hand, the double-degenerate scenario will not give rise to any circumstellar medium close to the progenitor system, and hence essentially no prompt radio emission is expected. Nonetheless, we note that the radio emission increases with time in the double-degenerate scenario, contrary to the single-degenerate scenario. This also opens the possibility for confirming the double-degenerate channel in Type Ia SNe via ultra-sensitive radio observations of decades-old Type Ia SNe. The best constraints on the mass-loss rate from Type Ia SNe come indeed from radio interferometric observations of SN 2011fe (e.g. Chomiuk et al. 2012), using the VLA, and of SN 2014J (Pérez-Torres et al. 2014; see also Fig. 4.2).

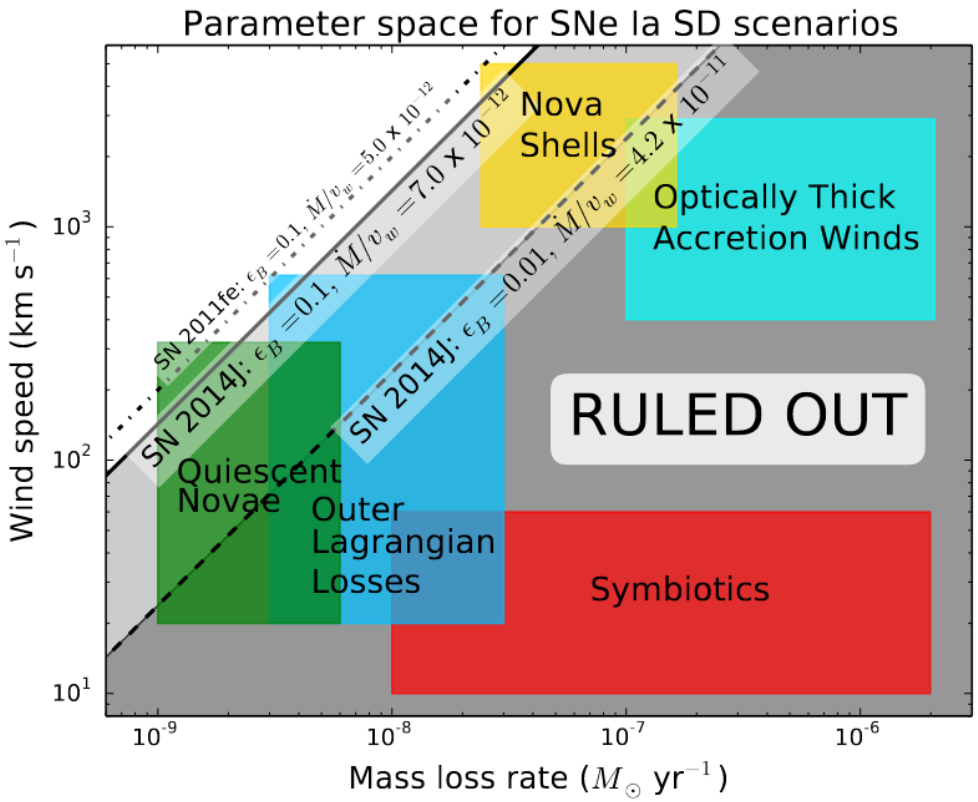

Figure 4.2: Constraints on the parameter space (wind speed vs. mass-loss rate) for single degenerate scenarios for SN 2014J. Progenitor scenarios are plotted as schematic regions. We indicate our 3σ limits on $\dot{M}/v_w$, assuming $\varepsilon_B = 0.1$ (solid line) and the conservative case of $\varepsilon_B = 0.01$ (dashed line). Mass loss scenarios falling into the gray-shaded areas should have been detected by the deep radio observations, and therefore are ruled out for SN 2014J. For comparison, we have included also the limit on SN 2011fe (dash-dotted line) for the same choice of parameters as the solid line for SN 2014J, which essentially leaves only room for quiescent nova emission as a viable alternative among the single-degenerate scenarios for SN 2011fe (Pérez-Torres et al. 2014). ©AAS. Reproduced with permission.

Unfortunately, the volumetric rate of Type Ia SNe is rather small, $\sim 3 \times 10^{-5}$ SN yr^{-1} Mpc^{-3} (Dilday et al. 2010). Therefore we should expect to have on average about 1 SN Ia every year within a radius of 20 Mpc. This illustrates two things: first, the crucial point of following each and every SN Ia that happens to explode nearby, as each one represents a unique opportunity. For example, SN 2011fe in M51 ($D \approx 7$ Mpc) and SN 2014J in M82 ($D \approx 3.8$ Mpc) yielded upper limits to the mass-loss rate of any putative non-degenerate companion of $\lesssim 5 \times 10^{-9}$ $M_\odot$ yr^{-1}and $\lesssim 7 \times 10^{-9}$ $M_\odot$ yr^{-1}, respectively. Those constraints are about two orders of magnitude deeper than probed by all previous radio interferometer observations together.

While VLA-like radio interferometers are more sensitive than the EVN, the latter will continue to play a very important role in those studies, thanks to its mas-angular resolution, which filters out the diffuse emission.

4.1.3 Core-collapse supernovae and long gamma-ray bursts

Core-collapse supernovae

The discovery of an expanding radio shell in SN 1993J (Marcaide et al. 1995a) using global VLBI, beautifully confirmed theoretical expectations (Chevalier 1982) for core-collapse supernovae (CCSNe) and opened an avenue for detailed studies of the supernova-circumstellar medium interaction, and the (direct) measurement of the supernova radius and its expansion speed as a function of time has implications on both the CSM and the progenitor's ejecta density profiles (Chevalier 1982).

However, so far only a handful of CCSNe have been imaged with enough detail as to make significant progress, including SN 1993J, a Type IIb SN, still being the best studied case after 25 years (Marcaide et al. 1995a,1995b,1997; Martí-Vidal et al. 2011a,2011b), SN 1979C (Marcaide et al. 2009), SN 1986J (Pérez-Torres et al. 2002), SN 2001gd (Pérez-Torres et al. 2005), SN 2008iz (Brunthaler et al. 2010).

With increased sensitivity and better *uv*-coverage provided by the growing number of antennas, the EVN should be able to probe the SN-CSM interaction for all CCSN types, from the relatively faint Type IIP to the extremely radio bright Type IIn SNe in the local Universe, via directing VLBI imaging of those SNe. Probing the SN-CSM interaction for all CCSN types will allow us to obtain basic, crucial information to characterise their progenitors, including the following: (i) pre-supernova mass-loss rates; (ii) shock radius measurements and radius evolution, allowing to study the different regimes of deceleration in the expansion, and whether self-similar expansion applies, or not; (iii) estimate the magnetic field–directly from VLBI observations–for synchrotron self-absorbed SNe.

Another relevant, yet poorly known aspect in supernova studies is (iv) the transition from (young) supernova to supernova remnant, i.e. the passage from a phase where the emission is driven by the interaction of the SN ejecta with the circumstellar medium to a phase where the radio emission is driven by the interaction with the ISM. To understand better that important phase in the lifes of SNe, we necessarily require long-term monitoring programmes to trace those changes in detail.

Finally, EVN observations of CCSN factories in the central regions of starbursts have yielded a unique opportunity to track the evolution of large amounts of CCSNe (e.g., Parra et al. 2007, Pérez-Torres et al. 2009, Batejat et al. 2011, Bondi et al. 2012, Varenius et al. 2019), compared the more focused, individual studies of SN, at the expense of missing the opportunity of directly imaging their expansion. However, advances in the modelling of the *uv*-data, which carries this fundamental information, is overcoming this limitation (e.g. Marti-Vidal et al. 2012), and will be probably the way to go forward.

In short, even after the advent of SKA1, the use of the EVN, whether as a standalone array, or as part of a global VLBI array, including MeerKAT as a a phased-array, will be crucial to attain the milliarcsecond angular resolution, a mandatory requirement to reach any of the above stated goals. Thanks to the slow evolution of CCSNe (essentially all type IIn, IIL, IIP, IIb SNe), the fact that the EVN does not have multi-frequency simultaneous capabilities is not a dramatic issue, but it must be recognised that this is a drawback, and a serious limitation for studies of the fast evolving CCSNe (Type Ib and Ic SNe). The existence of the e-EVN has improved the serious limitations that the EVN had in those studies, allowing to point to a "good" VLBI CCSN candidate ($D \lesssim 30$ Mpc) within one-two weeks from its explosion, and permitting for a reasonable monitoring of its evolution.

Long gamma-ray bursts

It is now widely accepted that long-duration GRBs are ultra-relativistic jets marking the deaths of a certain subset of massive stars. Since the discovery of the GRB–associated supernova (SN) 1998bw (to Galama et al. 1998), about a dozen core-collapse SNe have been identified in connection with

GRBs (Modjaz et al. 2016). Intriguingly, all GRB-associated SNe discovered thus far are classified as type Ic with broad lines (BL-Ic), establishing a relationship between GRBs and BL-Ic events (Woosley et al. 2006). According to the fireball model (Piran 1999), for every GRB we see in γ-rays there should be $\sim 10-100$ more that launch misaligned jets and are missed at high energies, called off-axis GRBs. If an off-axis GRB went off relatively nearby, we would expect light from the associated BL-Ic SN to be visible initially, followed by an off-axis jet emerging as a strong radio source at later times, when the jet decelerates, spreads, and intersects our line of sight (Figure 4.3, panel C; see also Nakar & Piran 2003).

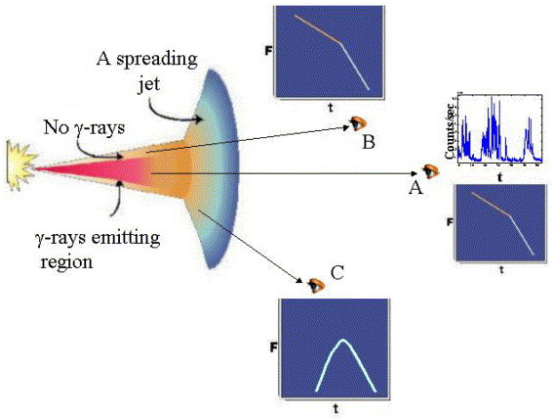

Figure 4.3: Observing long-GRB jets. Observer A is on–axis and detects the GRB and its afterglow. Observer B is on–axis but outside the gamma-ray emitting region, and detects an on–axis orphan afterglow similar to observer A. Observer C is off–axis (i.e. outside the initial jet opening angle) and detects a radio off–axis orphan afterglow that rises and falls and differs from the afterglow detected by observers A and B. Figure from Nakar & Piran (2003).

However, after more than 20 years since the discovery of GRB afterglows, we have, not yet been able to find an off-axis GRB associated with a BL-Ic SN. VLBI observations of long-GRBs are particularly useful, as they provide an extremely accurate and precise location of the GRB afterglow, as well as to monitor how the expansion proceeds. Direct size measurements with VLBI can also provide crucial information on the jet dynamics, in particular the sideways spreading of the jet. While it is well known what happens at early times when the jet is ultra-relativistic, and at late times when the outflow is non-relativistic and quasi-spherical; but what happens in between those two stages is less well established. In early GRB studies, it was assumed that the sideways spreading of the jet was very fast (e.g. Rhoads et al. 1999), but hydrodynamics simulations have shown that the sideways spreading is more gradual (e.g. Zhang & MacFadyen 2009). This is still a point of debate in the GRB community, and can probably only be resolved by accurate VLBI measurements of GRBs (see also Granot and van der Horst 2014).

VLBI observations can also provide crucial information to discern among the GRB scenarios at work, in particular to disentangle whether the GRB ejecta interacts with a steady circumstellar wind ($\rho \propto r^{-2}$), or with a constant density ISM.

Some SN Ic-BL show more than one peak in its radio luminosity curve. This behavior can be due most likely to either extreme CSM density variations, or to an emerging off-axis GRB. In the varying

density scenario, a spherical SN shock powers the radio emission, and the double-peaked radio light curve would be due to density variations in the CSM, perhaps related to eruptive progenitor mass loss (e.g., Soderberg et al. 2005, Wellons et al. 2012, Salas et al. 2013, Corsi et al. 2014, Milisavljevic et al. 2015). In the emerging off-axis GRB, the radio emission observed during the first peak is produced by the spherical SN shock, while the second radio peak corresponds to the emerging off-axis jet initially pointed away from our line of sight (Fig. 1, panel-C).

The above scenarios make rather different predictions for the angular diameter size of the GRB at (very) late times. For example, for the case of PTF 11qcj, its angular diameter will reach ≈ 1 mas around 2500 days post explosion (Palliyaguru et al. 2020). A much larger angular diameter of ≈ 25 mas is instead expected for an off-axis jet at the same epoch. Therefore, VLBI observations of those GRBs are the only possible way to remove model degeneracies, which are left open by radio light curve monitoring, and ultimately test for the presence of an off-axis jet in this BL-Ic SN. We note that all previous claims of off-axis GRB jet discoveries have indeed been ruled out via VLBI angular diameter measurements (e.g., Granot & Ramirez-Ruiz 2004, Bietenholz et al. 2014). Thus, this method has proven to be extremely effective in the few cases so far observed.

4.1.4 Tidal disruption events

Tidal disruption events (TDEs) are transient flares of electromagnetic radiation produced when a star is ripped apart by the gravitational field tides of a supermassive black hole (SMBH; Rees 1988). During the disruption, one fraction of the stellar debris is ejected, whereas the remaining fraction is accreted onto the SMBH, generating a bright flare that is normally detected in the X-ray, UV, and optical part of the spectrum (see, e.g., Komossa 2015 for a review). Early theoretical models of tidal disruptions predicted the accretion rate onto the SMBH and consequently, the tidal disruption flare decay with characteristic time dependence $L \propto t^{-5/3}$ (Rees 1988; Evans & Kochanek 1989). Subsequent studies have found deviations from this power law dependence for different stellar structure of disrupted stars and different initial orbits (Lodato et al. 2009; Guillochon & Ramirez-Ruiz 2013).

In addition to these thermal signatures, some TDEs show evidence for existence of powerful relativistic jets (Burrows et al. 2011; Levan et al. 2011; Zauderer et al. 2011; Bloom et al. 2011; Cenko et al. 2012). Jetted TDEs are expected to produce associated radio transients, lasting from months to years, and form an important population which can be used to study the formation and evolution of relativistic jets in otherwise dormant SMBHs (Giannios and Metzger 2011).

Indirect evidence of such a putative radio jet has been inferred for *Swift* J1644+57 (e.g. Mimica et al. 2015), but the source remains unresolved with VLBI; ultra-precise EVN astrometry constrained the apparent ejection velocity to less than 0.3c, averaged over three years (Yang et al. 2016). ASASSN-14li was another case where indirect evidence pointed to a radio jet (van Velzen et al. 2016), although the nature of the radio emission from this object is controversial, with others interpreting it as being due to a disk wind (Alexander et al. 2016). EVN observations of ASASSN-14li (Romero-Canizales et al. 2016) resolved the radio structure into two components, but the interpretation of the observations was also inconclusive. The direct confirmation of a TDE radio jet has therefore remained elusive until very recently, when Mattila et al. (2018) detected a milliarcsecond-long radio jet in the dust-enshrouded TDE Arp 299-B AT1 in the nearby (D=45 Mpc) galaxy merger Arp 299 (see also Fig.4.4). The role of the EVN in this study was crucially important.

The gravitational field of the SMBH in Arp 299-B, with a mass 20 million times that of the Sun, shredded a star with a mass more than twice that of the Sun. This resulted in a TDE that

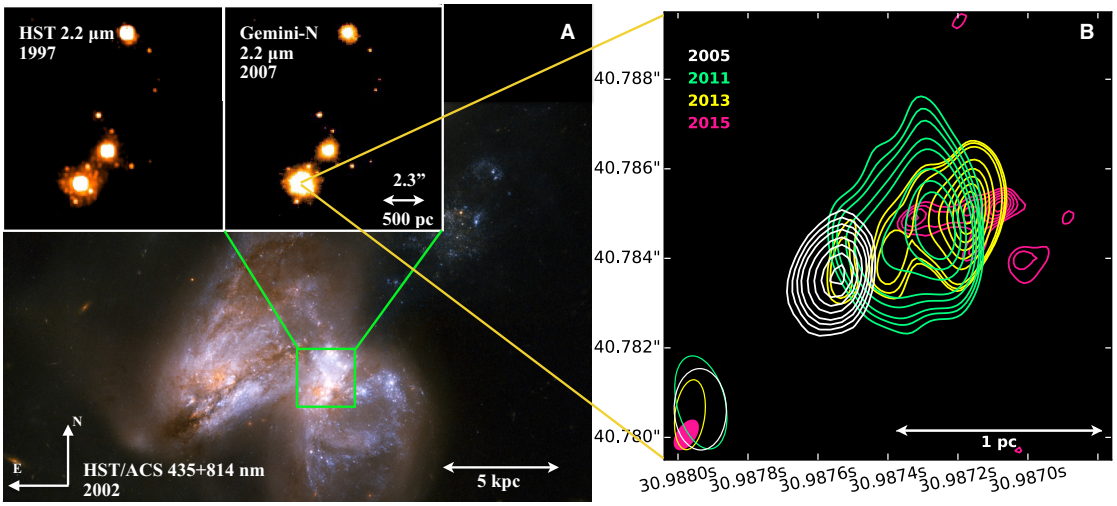

Figure 4.4: The transient Arp 299-B AT1 and its host galaxy Arp 299. **(A)** A colour-composite optical image from the *HST*, with high-resolution, 12.5 by 13 arcsec size near-IR 2.2-mm images [insets **(B)** and **(C)**] showing the brightening of the B1 nucleus (7). **(D)** The evolution of the radio morphology as imaged with VLBI at 8.4 GHz [7 $\times$ 7 milli-arcsec (mas) region with the 8.4-GHz peak position in 2005, right ascension (RA) = 11h28m30.9875529s, declination (Dec) = 58°33'40".783601 (J2000.0)]. The VLBI images are aligned with an astrometric precision better than 50 mas. The initially unresolved radio source develops into a resolved jet structure a few years after the explosion, with the centre of the radio emission moving westward with time. The radio beam size for each epoch is indicated in the lower-right corner. From Mattila et al. (2018), Science.

was not seen in the optical or X-rays because of the very dense medium surrounding the SMBH, but was detected in the near-infrared and radio. The soft X-ray photons produced by the event were efficiently reprocessed into UV and optical photons by the dense gas, and further to infrared wavelengths by dust in the nuclear environment. Efficient reprocessing of the energy might thus resolve the outstanding problem of observed luminosities of optically detected TDEs being generally lower than predicted.

The case of Arp 299-B AT1 suggests that tidal disruptions of young, massive stars may be relatively common. However, events similar to Arp 299-B AT1 would have remained hidden within dusty and dense environments and would not be detectable by optical, UV or soft X-ray observations. Such TDEs from relatively massive, young stars might power strong AGN radiative feedback, especially at higher redshifts where galaxy mergers and luminous infrared galaxies like Arp 299 are more common.

The role of the EVN in TDE studies: Lessons learned and caveats.

1. The combination of high-angular resolution near-IR and radio observations will allow for many new discoveries that are hidden by a curtain of dust, so missions like WISE, and radio interferometric arrays like SKA (with baselines of several thousands of kilometres) will result in many more discoveries than in the optical, UV, or X-rays.
2. Direct probing of the formation and evolution of radio jets in TDEs necessarily requires VLBI monitoring of TDE candidates, at high-dynamic range and deep sensitivities.

3. The astrometric capabilities of the EVN are, and will be, crucial for those studies, as the location and motion of a putative TDE jet requires position milliarcsecond accuracies and angular resolutions, or even better, as shown in the cases of *Swift* J1644+57 (Yang et al. 2016) and Arp 299B-AT1 (Mattila et al. 2018).
4. The role of the e-EVN will increase, thanks to an increased cadence of the observations.
5. The bottleneck of the EVN to contribute in an unique way to this field are: (i) its lack of frequency agility, as has been the case since the very beginning of the EVN; (ii) the still rather inhomogenous frequency setup offered by the array, which significantly complicates interpretation.

4.1.5 Neutron star and black hole mergers, and gravitational waves

With the discovery of mergers of binary black holes (Abbott et al. 2015), the new era of gravitational wave astronomy started. Soon after the discovery of the first merger of two binary neutron stars GW/GRB 170817 (Abbott et al. 2017b) signed the start of the multi-messenger astronomy era due to the detection of the electromagnetic emission shortly following the gravitational signal (Abbott et al. 2017a).

GW/GRB 170817 showed three types of electromagnetic emission components:

1. two seconds after the gravitational event, detected by LIGO/Virgo (see e.g. Abbott et al. 2017b and references therein), a weak short duration γ–ray burst triggered *Fermi* (Goldstein et al. 2017) and INTEGRAL (Savchenko et al. 2017). Its temporal and spectral features resembled those of short Gamma Ray Bursts (GRB), expected to arise from a binary compact object merger;
2. less than 11 hours later a bright optical counterpart was discovered (Coulter et al. 2017) in the outskirts of the faint host NGC 4339 at 40 Mpc. Follow up observations of this thermal optical/near-IR emission component over the next 25 days showed a fast decline compatible with the emission from the radioactive decay of the heaviest elements produced by rapid neutron capture in the merger ejecta. About 0.05 $M_\odot$ neutron rich material was ejected in the merger (Pian et al. 2017).
3. starting 10 days post merger and up to more than a year after the merger long–lived non–thermal emission component was detected from the X-ray through the optical to the radio band (e.g. Margutti et al. 2018, Hajela et al. 2019). This was interpreted as the afterglow produced by the (collimated ?) relativistic outflow.

If, similarly to other bright short and long GRBs, the γ–ray emission of GRB 170817 were produced by a relativistic jet of few degrees aperture ($\sim$5-10°), given the small distance to the source, it should be misaligned ($\sim$20°) with respect to the line of sight. This would account for the observed isotropic equivalent luminosity $L_{\rm iso} \sim 10^{47}$ erg s^{-1} which is four orders of magnitudes smaller than ever measured for cosmological short GRBs. Alternatively, such a low luminosity could be due to a mildly relativistic, nearly isotropic, outflow either produced by the neutron stars' magnetic field (Salafia et al. 2018) or by the interaction of the jet with the merger ejecta. In the latter case, the jet deposited all its energy in the expanding ejecta (choked jet) producing an expanding nearly isotropic mildly relativistic outflow (cocoon).

These two models, different for their geometric and dynamical properties (relativistic narrow jet versus mildly relativistic nearly isotropic outflow), have been competing for almost three months until the intense radio monitoring (Mooley et al. 2018a - confirmed also by X–ray and optical observations - Margutti et al. 2018) showed that the afterglow luminosity increased slowly ($\propto t^{0.8}$)

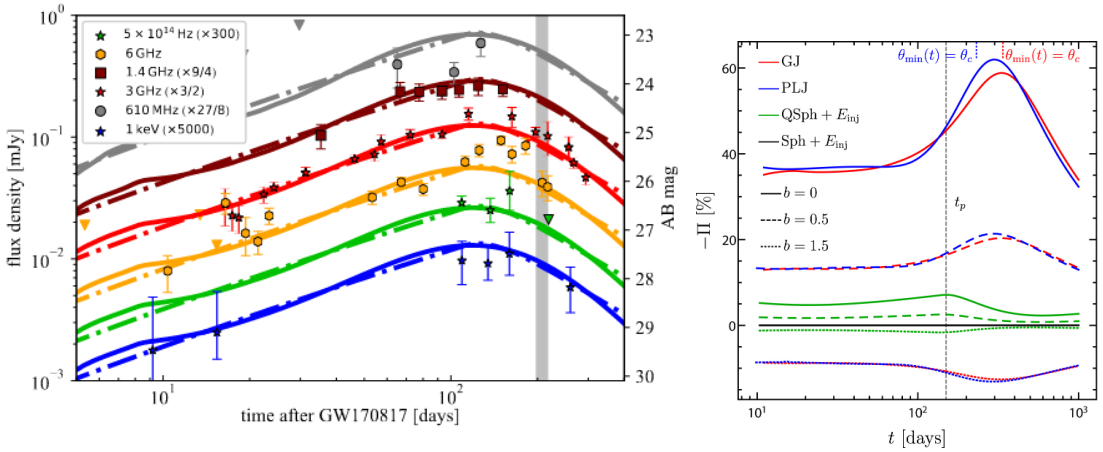

Figure 4.5: (left) Light curve at different frequencies (re-scaled as shown in the legend) with the two competing models (adapted from Ghirlanda et al. 2019): a relativistic jet with an angular distribution of energy and bulk velocity (structured jet - dot–dashed line) and a nearly isotropic mildly relativistic jet with a radial stratified structure in bulk velocity (cocoon - solid line). (right) Linear polarisation as a function of time (Fig. 7, Gill & Granot 2018) for different geometric configuration of the outflow (GJ=Gaussian Jet, PLJ=Power–Law Jet, QSph=Quasi Spherical outflow with energy injection and Sph=Sperical outflow) and different configuration of the magnetic field (b=0 aligned with the shock plane and no component perpendicular to the shock plane.

and finally peaked ∼200 days after the event reaching flux densities of ∼100μJy at 6 GHz (Mooley et al. 2018c)[1]. This led to a substantial modification of the above scenarios, which would produce a much steeper luminosity rise, allowing for an angular structure of the jet energy and bulk velocity (structured jet model) or for a radial distribution of the expansion velocity within the cocoon.

The angular structured jet (dot–dashed line in Fig.1) and the dynamically structured cocoon (solid line in Fig.1) , however, are compatible (for some sets of parameters) with the observed light curve and cannot be distinguished with multi-wavelength photometry alone.

The different nature of the structure could be distinguished through radio observations providing:

- *continuum polarisation*: a large degree of linear polarisation (≈20%) would indicate a high level of asymmetry, favouring a jet scenario (e.g. Rossi et al. 2004; Nakar et al. 2018). However, polarisation is determined by (i) the geometry of the outflow and (ii) the magnetic field configuration. JVLA observations (at 2.8 GHz) of GRB 170817 240d after the merger (Corsi et al. 2018) rule out linear polarisation larger than 12% (99% confidence level). This result can still be compatible with the structured jet scenario if the magnetic field in the emission region has, also, a component perpendicular to the shock plane (e.g. Gill & Granot 2018 - Fig.4.5, right panel);
- *imaging*: due to its larger expansion velocity and being more collimated with respect to the cocoon, a relativistic narrow jet should produce (e.g. Zrake, Xie & McFadyen 2018 - Fig.4.6) a larger apparent displacement and a smaller size (more compact source). The projected position (with respect to the explosion site) in the plane of the sky of a relativistic jet should

[1]The spectral energy distribution from the X–ray to the radio is consistent with synchrotron emission from shock accelerated electrons (Margutti et al. 2018).

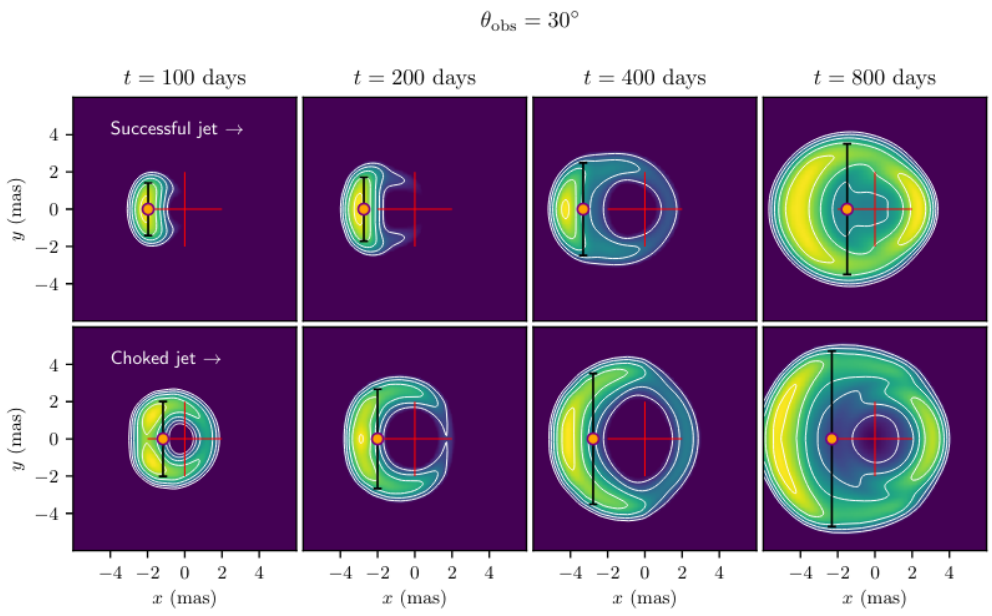

Figure 4.6: Radio images of the structured jet model (top panels) and of the choked (or cocoon) model (bottom panels) at different epochs with respect to the explosion time. The site of the explosion is marked by the red cross (2 mas in size) and the surface brightness (colour coded) spans four orders of magnitudes. The orange dot show the centroid of the surface brightness and the vertical black bar its FWHM (Zrake, Xie & McFadyen 2018). ©AAS. Reproduced with permission.

be larger than that of the cocoon (eventually with no displacement in the case of a completely symmetric isotropic outflow). VLBA observations (Mooley et al. 2018b) of GRB 170817 showed that its apparent motion is consistent with the predictions of a relativistic structured jet (Fig.4.7 - left panel). A source size (Fig.4.7 - right panel) smaller than 2.5 mas at 207 days obtained through global VLBI observations (Ghirlanda et al. 2019) probes that a relativistic jet emerged from the BNS ejecta.

The reprise of the advanced LIGO and Virgo observing run O3 will offer the opportunity to combine these probes (continuum polarisation measurements and high resolution imaging). The brightness of the new events will be influenced by several factors like the density of the circumburst medium or the jet orientation and the global energy in the relativistic ejecta. Also the polarisation evolution (Fig.4.5 - right) will depend on the jet geometry and on the magnetic field configuration. Polarisation constraints below 10%, attainable with the VLA with events as luminous as twice GRB 170817 at its peak (Corsi et al. 2018), are expected to challenge the jet scenario (Fig.4.5, right panel). However, if a jet is present, such constraints would probe the magnetic field configuration in the emission region. Independent probes of the outflow properties will be provided by high resolution imaging of the source as was the case of GRB 170817 (Mooley et al. 2018b; Ghirlanda et al. 2019). There are great expectations also for the possible first detection, in O3, of BH-NS merger events whose electromagnetic emission is still completely unexplored. The EVN can contribute in exploiting the wealth of information attainable through observations in the GHz range: radio continuum flux measurements can trace the temporal evolution of the flux and, in concert with other wavelengths, e.g. optical and X-ray, to probe the broad band SED and the emission regime of the

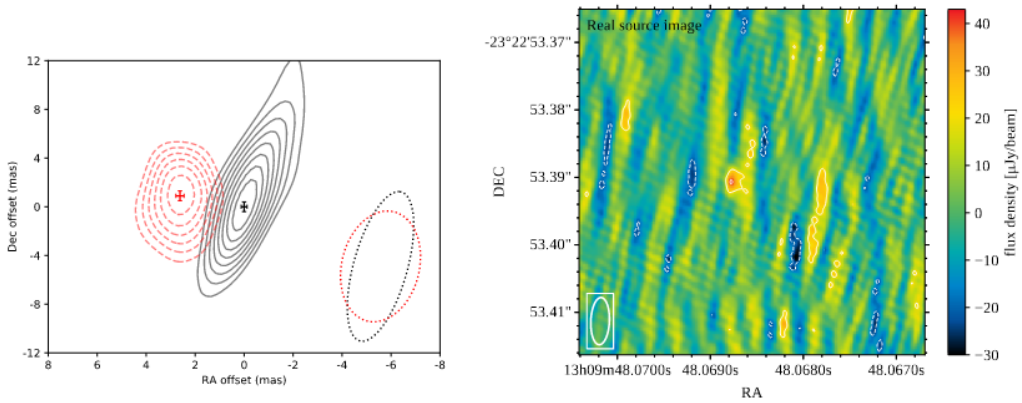

Figure 4.7: (left) Source position at 75d and 230d showing an apparent displacement of 2.7±0.3 mas. The bottom right corner shows the synthesised beam size of the two epochs (Mooley et al. 2018b). (right) Source image at 207 days obtained through global VLBI observations (Ghirlanda et al. 2019).

non–thermal component produced by the deceleration of the relativistic outflow.

4.2 Fast transients

A relatively unexplored part of the radio transient parameter space is a phenomena collectively called fast transients. These are very difficult to detect because they have durations much smaller than the typical integration times of a few seconds in most common VLBI applications, and in general they are not trivially distinguished from RFI. They originate in coherent processes and their brightness temperatures may therefore well exceed the inverse-Compton limit for incoherent transients. These short pulses or flares are dispersed by the ionised medium as they travel through it towards the observer. In most cases these can only be detected once the data have been dedispersed to a broad range of dispersion measures (DM); having to search DM-space is one of the reasons why finding fast transients is challenging.

4.2.1 Fast radio bursts

The FRB phenomenon

The first fast radio burst (FRB), was found in a Parkes pulsar-search data base after an algorithm optimised for finding single pulses using a matched filtering technique was run up to very high DM values. FRB 010824 had a dispersion measure value well in excess of the typical line-of-sight Galactic DM in that direction, and therefore was assumed to be extragalactic (Lorimer et al. 2007). This was followed by a number of other detections (e.g. Thornton et al. 2013), but understanding the nature of FRBs was not possible because single dish detections provide only very poor localisation, down to a few arcminutes at best.

Measuring the DMs for hundreds of FRBs and the redhsifts of their hosts would have a profound impact on cosmology, as it would reveal the baryon distribution in the Universe within redshift of $z \sim 1$ (Macquart et al. 2015). One may constrain the dark energy equation-of-state parameter using FRBs at even higher redshifts, where the DMs are dominated by the IGM (Zhou et al. 2014). Finally, the intergalactic magnetic fields could be constrained from the rotation measure and scattering of

FRB signals (Macquart et al. 2015). FRB detection and localisation is one of the highest-ranked high priority science objectives of the SKA, in which therefore VLBI may play a key role, because $< 0.5''$ localisations will be necessary for secure dwarf galaxy host identifications at redshifts $z > 0.1$ (cf. Eftekhari & Berger 2017).

The VLBI data are usually heavily averaged in time and frequency that smears out the signal, and also reduces the field of view drastically. Because of the very short duration, traditional VLBI follow-up observations of single pulses are not possible either. The solution is to apply wide-field techniques and find repeating FRBs that can be followed-up at high resolution. The basic scheme of using the e-EVN for single-pulse localisation and the related LOCATe project work was outlined by Paragi (2017). Around the same time, the first repeating fast radio burst was found at Arecibo (Spitler et al. 2016). FRB 121102 was successfully localised with the JVLA (Chatterjee et al. 2017, $\sim$100 mas precision) and the e-EVN (Marcote et al. 2017, $\sim$10 mas accuracy) within a year of the discovery of its repeating nature. A large number of FRBs have been discovered with ASKAP (Shannon et al. 2018) and CHIME (Amiri et al. 2019) in the following few years. Sub-arcsecond localisation have only been possible for a few cases (Bannister et al. 2019 and Prochaska et al. 2019 with ASKAP; Ravi et al. 2019 with the DSA-10), and the only other mas-precision result was for a second repeater FRB 180916.J0158+65, found by CHIME and localised with the EVN (Marcote et al. 2020).

In the first ten years of FRB research there have been more models proposed to explain the phenomenon than detected FRBs. The first localisation shed light on the extragalactic origin of FRB 121102, which reduced the number of competing models significantly. This is however just the beginning of the story: we still do not know if there are multiple populations of FRBs, and what their true nature is. To be able to reveal their possible progenitors, many more FRB localisations are necessary with interferometers than the above mentioned few cases. In the case of FRB 121102 the host is a metal-poor dwarf galaxy, also typical site for long-GRBs and superluminous supernovae (Tendulkar et al. 2017). The milliarcsecond localisation with VLBI, together with high-resolution optical imaging indicated that it originates in a star forming region within the host galaxy (Bassa et al. 2017). The three localised single-pulse FRBs were related to massive galaxies with little or no star formation, while the second localised repeater was found in a spiral galaxy (Marcote et al. 2020).

Meeting the challenge of detecting short-duration, dispersed astronomical signals will have a major impact on astronomy and possibly beyond, just like in the early days of research into calibrating radio interferometry data and detecting the Hawking-radiation influenced the development of Wi-Fi. FRB searches in VLBI data will be a driver for other developments, because it requires high time/frequency correlation to meet the requirements for finding very short duration, dispersed signals in a large FoV, but at the same time providing very high angular resolution. This science case pushes along all axes of parameter space, which will be beneficial for other applications as well. In addition, it will have an impact on the design of future telescopes, data acquisition systems, search algorithms (machine learning?), RFI detection, and the way we are looking at 'big data' problems. There is considerable synergy between the FRB field and SETI, which has a broad societal impact (e.g. Siemion et al. 2013; see section 4.2.3).

Fast transient research with the EVN

The $logN - logS$ distribution of the FRB population is still not known, but the latest research indicates that there may be an FRB in the sky every minute detectable by SKA sensitivities (Fialkov & Loeb 2017). The EVN can make a significant contribution by characterising the known FRB hosts

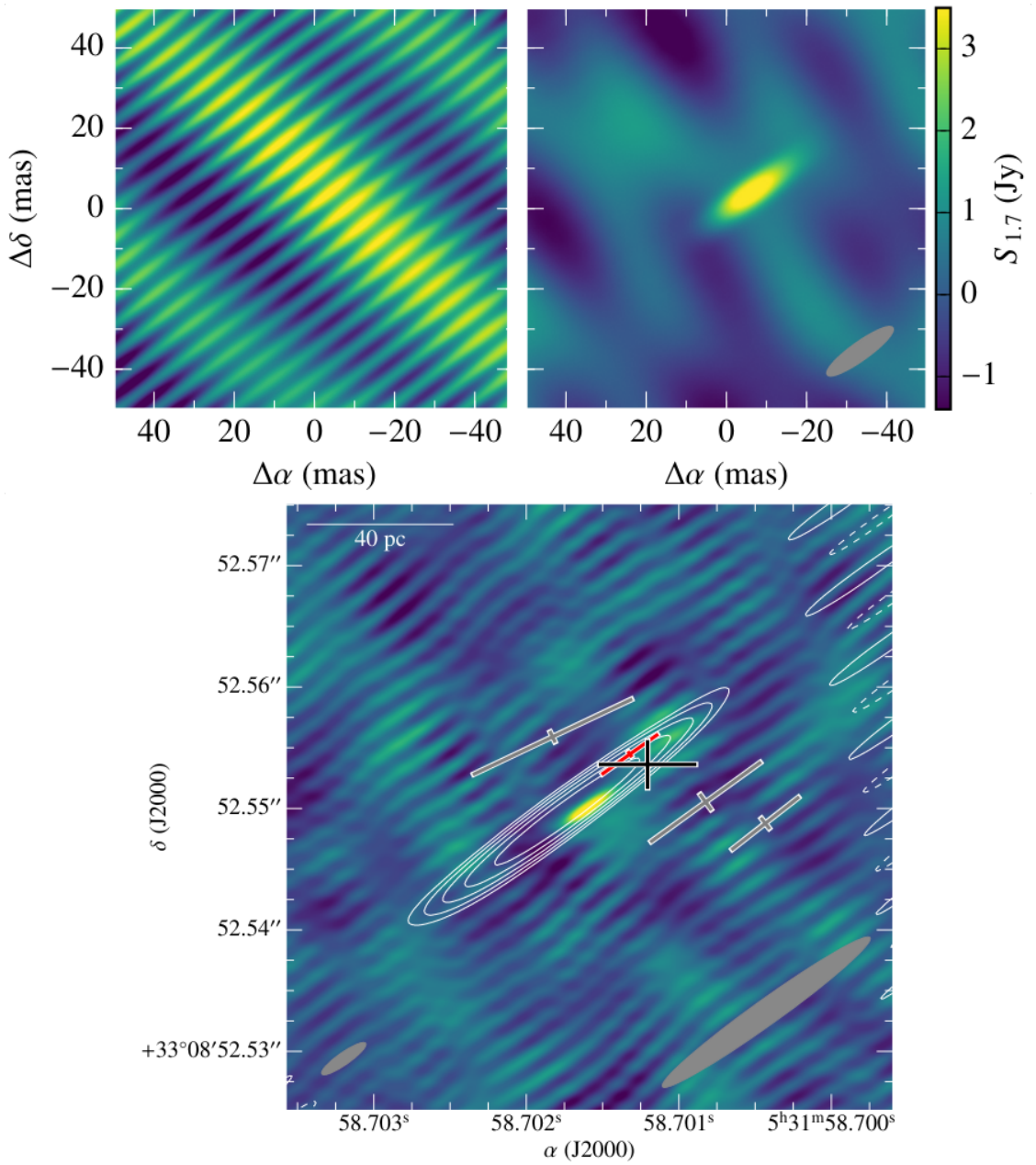

Figure 4.8: (upper panel) The dirty (left) and clean (right) maps of the brightest pulse from FRB 121102 on 20 September 2016. The limiting *uv*-coverage in VLBI observations has an even higher impact on very short snapshot imaging. In this particular case the dominance of Arecibo baselines is clearly visible. (lower panel) The positions of all four pulses detected in the same experiment with their error estimates (red: brightest; black: weighted mean), overlaid on the clean map of the compact, persistent radio source found coincident with FRB 121102 (Marcote et al. 2017). ©AAS. Reproduced with permission.

(requiring regular VLBI), getting refined positions of repeating sources (in custom experiments), and detecting/localising unique new single-pulse events (a commensal approach is needed: e.g. Burke-Spolaor et al. 2016; Paragi 2016). The former two should be possible for up to dozens of new FRBs during the next decade, assuming new discoveries will come in great numbers. The chances for unique single pulse detections are less clear.

The major limitation of current instrumentation for FRB searches is the low survey speed for fast transients[2], and it is related to the fact that most of the EVN sensitivity comes from great dishes that limit the field of view. Also, while single-pulse FRBs are not very broad band, pulses may appear at a broad range of frequencies (Gajjar et al. 2018) therefore having narrow band receivers limits the chances of detection. The usual 2-bit sampling employed in VLBI systems limits the dynamic range for single pulses and makes fighting the RFI more difficult, although for the latter there are promising new methods (e.g. Nita et al. 2019). Other limitations include poor instantaneous *uv*-coverage, issues with formatting VLBI data, automatic gain control and T_{sys} measurements (Paragi 2016; Huang et al. in prep.).

The unique capability of the EVN for FRB research is that it combines a collective area that of the planned SKA1-MID with very high angular resolution. To detect short bursts collecting area is very important, since one cannot win extra sensitivity by increasing the observing time. The current fluence detection limit with the greatest telescopes is $\sim$0.1 Jy ms, i.e. a few hundred mJy peak flux density for a millisecond-duration event – for FRB 121102, three out of the four e-EVN-detected pulses could not have been found without Arecibo. So far it has also been an advantage that some of the largest dishes that are member of the EVN have had dedicated (broad-band, high-bit-sampling) pulsar backends to support FRB observations. The flexibility offered by the regular e-EVN sessions was also a plus to be able to carry out monitoring observations of FRB 121102, hoping to catch active periods. The flexibility of the EVN SFXC correlator (Keimpema et al. 2015) for doing wide-FoV style correlation of very short time samples, and the SFXC implementation of coherent dedispersion capability was also essential[3].

Requirements and synergies

The characterisation of the FRB host galaxies – to better constrain the environments of FRB progenitors – requires a multi-band approach. It mainly implies studying the star formation and AGN activity in the host, and especially near the FRB position. The host of FRB 121102 is a metal-poor dwarf galaxy at a redshift of $z = 0.1927$. It has an off-nuclear persistent, compact radio source of ~ 180 μJy coincidental with the FRB position, representing either a magnetar-powered pulsar-wind nebula, or low-luminosity AGN activity. The observed extremely high RM of $\sim 10^5$ radians per square metre (found in the nearly 100% linearly polarised pulses of FRB 121102) have only been seen around (super-)massive black holes – while a scenario of a highly magnetised pulsar-wind nebula or supernova remnant surrounding a young neutron star still cannot be ruled out (Michilli et al. 2018). The persistent radio source may be a representative for a new source population well into the sub-mJy regime. To study this population in detail one just needs regular phase-referencing VLBI, but with μJy sensitivity and milliarcsecond resolution. To localise future known sources of repeating FRB pulses at mas resolution, one will need custom experiments in which e.g. Arecibo or Effelsberg

[2]The survey speed metric for fast transients is the product of the FoV and the limiting survey sensitivity S^n, where n is -1.5 for Eucledian Universe and no cosmological FRB evolution (Macquart et al. 2015).

[3]The e-EVN upgrade was one of the main requirements in the EVN2015 document. The development of the e-VLBI technique and the SFXC correlator in particular have been made possible by the EC-supported EXPReS and NEXPReS projects.

piggybacks on the VLBI observations with their pulsar backends. This is essential for optimal sensitivity single-pulse search for bursts. Real-time e-VLBI observations may be required to trigger on active periods of the sources, but the telescope voltage data has to always be recorded. Only this approach allows the FRB timestamp in the VLBI data to be de-dispersed and recorrelated. There is thus a lot of synergy with large single dishes (76m Lovell Telescope, 100m Effelsberg, 500m FAST etc.) or interferometers with PAFs (WSRT-APERTIF, ASKAP), as well as other dedicated FRB search engines (Molonglo Observatory Synthesis Telescope in Australia, and CHIME in Canada) and the SKA1-MID itself.

To summarise, the major requirements are the increase in sensitivity and instantaneous *uv*-coverage by adding new telescopes and significantly inrease the collecting area of the EVN. While increasing the bandwidth by using broad-band single-pixel feeds may have advantages for single pulse detection at higher frequencies (cf. Gajjar et al. 2018), increasing the collecting area will remain very important because both the pulses and the related persistent sources will likely have steep spectra and thus are more likely to be detected at lower frequencies. Flexibility for triggered observations is also very important. The optional switching off of the automatic gain control as well as the continuous Tsys, and good RFI mitigation would greatly improve the data quality for FRB-pulse detection with the EVN. A commensal, real-time detection pipeline (real-time during the correlation) might be considered for the EVN correlator in JIVE, but the majority of new FRB discoveries will be delivered by very large FoV custom FRB-search experiments. A large field of view EVN Archive, storing the raw data for all observations –at least for a prolonged period of time– might be highly useful. This would allow for new searches whenever new algorythms are being developed, with practically unlimited spectral resolution. While chances for detection is low, a wide-field EVN Archive would facilitate mas-localisation for single-pulse FRBs, and this approach seems to be the only way to associate single-pulse events to individual sources within the host, which is crucial for understanding the FRB progenitor population. In addition, it would allow for a direct VLBI measurement of the scatter-broadened size for a high-z FRB to characterise the IGM up to very high redshifts, which would be a major breakthrough. This also requires a robust amplitude calibration (at least to a few percent) and short spacings for the telescopes that provide the longest baselines for the EVN.

4.2.2 Neutron stars and pulsars

A new renaissance of pulsar research

Half a century after the original discovery, in the last decade pulsar and neutron star science produced more outstanding results than ever. For instance: the discovery of the most massive NSs (Demorest et al. 2010, Antoniadis et al. 2013, Linares et al. 2018), the most extreme relativistic pulsar binaries (Cameron et al. 2018, Stovall et al. 2018), the first multiple system including three compact objects (Ransom et al. 2014), the transitional millisecond pulsars (Papitto et al. 2013, Archibald et al. 2009), a radio magnetar very close to the Galactic centre (Mori et al. 2013, Eatough et al. 2013). Also, the success of many search experiments has more than doubled the number of known millisecond pulsars (MSPs), some of them became regular targets of the regional Pulsar Timing Arrays, as well as of the International Pulsar Timing Array (IPTA), established in 2011 with the primary aim of detecting gravitational waves in the nanoHz frequency regime by using repeated timing observations of a large ensemble of millisecond pulsars.

Building from this very successful decade, the perspectives for pulsar and neutron star research are extremely promising: in fact, it has been selected as key science for many planned large instruments, and most notably for SKA1 (Kramer et al 2015). In this framework, the slogan invoked

by the pulsar and NS community since the beginning of the pathway to SKA *"find them, time them, and VLBI them"* is more valid than ever. The use of the VLBI technique, and in particular the capabilities of the EVN, will play a unique complementary role for the full success of the foreseeable future experiments, by providing very precise astrometry, improved timing precision, as well as key information about the NS environment and the material along the line of sight. The study of NS dynamics in the Galaxy (via determination of the proper motion of many targets, including the large number of slow pulsars), detailed imaging of the Pulsar Wind Nebulae in search for the occurrence of possible jets (via application of pulsar gating to subtract the strong pulsar signal and thus unveil either the termination shock or putative jets), and the investigation of the location and properties of the radio emission in NS binaries (via high resolution imaging) are some well known examples of NS science made possible by VLBI.

Prime goals for very high resolution pulsar science

1. Some relativistic binaries (e.g. the B1534+12 and the double pulsar systems) have precision tests of general relativity and alternate gravity theories limited by our inability to correct for kinematic effects and/or by poorly constrained distances. This limitation will become more and more important in the next decade, when the quality of the timing observations will be strongly enhanced by the availability of new large telescopes. In fact, although pulsar timing can directly provide a value for the proper motion and the parallax, an increasing corpus of data is manifesting significant discrepancies among the astrometric parameters obtained by pulsar timing and more precise VLBI determinations, e.g. Deller et al. (2016) invokes the solar wind as a likely candidate for the timing model errors when looking at low ecliptic latitude pulsars. Precision timing, coupled with VLBI astrometry will finally enable tests of gravitational radiation emission theories at the $\sim$0.01% level.
2. Precise distances, provided by the EVN, in combination with accurate optical spectrometry (delivered by the new large telescopes which are at the design and/or construction phase, e.g. ELT), will be extremely beneficial in order to constrain the mass, radius and chemical composition of the companion (most often a white dwarf or a swelled main sequence star) to many binary neutron stars. An accurate determination of those parameters will enable strong constraints to theories of gravity and to nuclear physics, as well as providing key information for the study of the evolution of compact systems including a NS.
3. Detection of nanoHz gravitational waves (GWs) could occur within some years using observations of the already existent Pulsar Timing Arrays (PTAs), and all studies concur that is warranted by SKA1. The first detection(s) will result from the observation of the effects of the stochastic GW background at the Earth. On a longer timescale, one will aim to also detect the effects of the GWs produced by single sources (e.g. Supermassive Black Hole Binaries, SMBHBs) at the location of (at least) a subset of the pulsars belonging to the PTAs. That will open up the intriguing possibility to strongly constrain both the sky location and the distance of the individual SMBHB (e.g. Deng & Finn 2011), whence the exciting chance to follow up the SMBHB in other electromagnetic bands. However, in order to achieve that, a very precise knowledge (of order $\sim 0.1 - 1.0$ pc) of the distance of the aforementioned subset of pulsars is required. Joint interferometric EVN-SKA1 (or EVN-MeerKAT) observations and/or interferometry of EVN telescopes combined with other very large instruments (e.g. FAST, ngVLA) will be suitable to deliver the best distance constraints. Besides improving on the achieved rms of the observations, such a high sensitivity system will allow one to also exploit relatively faint (< 1 mJy) in-beam calibrators, which should often be close enough on the sky

to the targeted pulsar. At the same time, the higher sensitivity will open the possibility to plan EVN pulsar observations at higher frequencies, thus strongly reducing the impact of the scattering, which is a serious issue at L-band for pulsars in the Galactic plane.

4. The quality of the timing data from a given pulsar typically scales linearly with the signal-to-noise of the collected signal profile. Therefore, the higher the sensitivity of the telescope is, the better the data are. A way to create very large (and highly sensitive) telescopes is to simultaneously operate many large dishes in tied-array mode. In pulsar research, this idea has been successfully implemented during past decade in the EU-funded LEAP project (Large European Array for Pulsars, Bassa et al 2016). This involves Effelsberg, Lovell, Nancay, Westerbork and Sardinia radio telescopes, the collecting area of which approaches that of a 200m dish, capable to observe a large portion of the sky. The perspective of adding most of the EVN dishes to the LEAP infrastructure, or of planning EVN+MeerKAT (or EVN+SKA1) tied-array observations, will create a fantastic instrument to perform ultra high precision timing for some tens of the most important targets.
5. Pulsar signals experience a full range of effects due to the intervening partially ionised medium: dispersion, scattering, refractive and diffractive scintillation, as well as Faraday rotation. Thus, single dish pulsar observations are known to be very effective tools for investigating the distribution of the ionised gas in the ISM and the Milky Way magnetic field. Their diagnostic capabilities grew with the discovery of the secondary spectrum *parabolic arcs* (Stinebring et al. 2001). In last decade, a new very powerful tool has been suggested, relying on VLBI observations of those parabolic arcs, via the so-called secondary cross spectra (Brisken et al. 2010). By using this technique, EVN observations (even better if combined with that of other large instruments, e.g. FAST, MeerKAT, SKA1, ngVLA) will allow one to potentially map the scattered brightness of a few pulsars with finer resolution (down to $\lesssim 100\mu$as) than the diffractive limit of the global instrument, shedding light on the sub-mas properties of the ISM along several lines of sight.
6. It has been recently shown that one can exploit the ISM as a giant lens, by performing VLBI imaging of the interstellar scattering speckle pattern associated with a very bright pulsar (a technique dubbed *pulsar VLBI-scintillometry*). It is expected (Pen et al. 2014) that the availability of future larger instruments in the VLBI network will provide the capabilities to measure the motion of the pulsar emission with sub-nanoarcsec accuracy, as well as enabling picoarcsec astrometry. This will improve the constraints on the still strongly debated size and height of the radio emission regions, as well as determine the size of the projected orbit for bright pulsars in binaries. This science case (as well as the one about the study of the ISM) is particularly tailored for VLBI at low frequencies, ~ 300 MHz.
7. In next decade there will be the possibility of exploiting the combined radio and optical emission from several binaries composed of a millisecond pulsar and a white dwarf in order to compare the astrometric coordinates derived by independently using the pulsar timing procedure, VLBI observations, and *Gaia* observations. That will lead (Paragi et al. 2015) to finally tie the three reference frames with better than 10 μas precision.

Technical requirements (pulsars)

To achieve these aims will require the EVN to: **(i)** increase the total sensitivity. That can be reached by including more telescopes in the array or by planning dedicated simultaneous observations with other high sensitivity instruments, and by widening the usable bandwidth. The aim should be 2 GHz of bandwidth, with dual pol and 2 bit sampling. That would deliver 16 Gbps, i.e. a factor of ~ 4

beyond what has been demonstrated at the moment, but it would technically be possible and would imply many benefits for pulsar-science; **(ii)** set up the correlator for enabling tied-array observations; **(iii)** ensure the availability of the pulsar gating mode, ideally with the capability of observing several pulsars at the same time, as for the many (sometimes tens of) millisecond pulsars included in a globular cluster. In this case, the visibilities should be simultaneously gated in pace with the ephemeris of each of the pulsars in the FoV; **(iv)** providing suitable frequency channelisation, in order to minimise the effects of the dispersion on the signal. In order to enlarge the circle of the users, it will be finally very important to provide and maintain public codes and pipelines for reducing pulsar-VLBI observations.

4.2.3 SETI

Over the last few years, the field of SETI (Search for Extraterrestrial Intelligence) has undergone a major rejuvination. The discovery by the *Kepler* mission that most stars host planetary systems, and that around 20% of these planets will be located within the habitable zone, plus the continually growing evidence that the basic pre-biotic constituents and conditions we believe necessary for life are common and perhaps ubiquitous in the Galaxy, has brought new focus to one of the most important questions that human-kind can ask itself - Are We Alone?

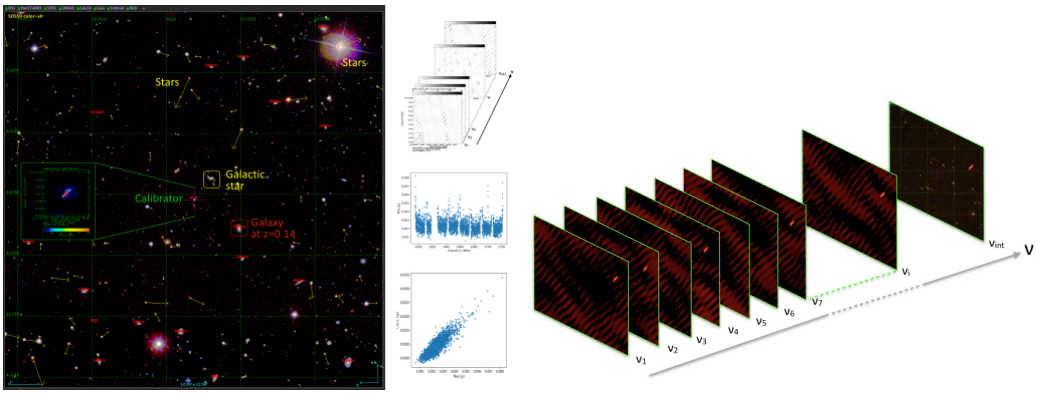

Figure 4.9: (left) The SDSS field centred on the calibrator J1025+1253, extracted from high time/frequency resolution EVN archive data. To the extreme right, the main results of searching for outliers in the 8192×32 kHz multi-channel images associated with a galactic star in the field. (right) The position of a SETI signal is likely to be invariant in its location on the sky. While everything else might be changing (e.g. central frequency and/or intensity with time) the signal location is expected to remain fixed, at least within the duration of a short observation. Credit: Garrett (2018).

One significant problem with all SETI searches to date (incl. the state-of-the-art Breakthrough Listen programme (Enriquez et al. 2017) is the number of false positives generated by both terrestrial radio frequency interference (RFI) and space-borne satellite communication systems. This is a situation that continues to grow steadily worse with time. Single dish telescopes are particularly vulnerable, compared to distributed arrays that can form an interferometer network. Interferometer arrays, such as the EVN/*e*-MERLIN, distributed on scales of 100-1000s of km are particularly good at suppressing RFI signals because the response to any signals arising outside of the relatively narrow field of view (e.g. any region outwith the primary beam response) decorrelate rapidly as one moves away from the correlated phase-centre of the observations (e.g. Rampadarath et al. 2012). Although

the SETI community has been reluctant to adopt interferometers as SETI search instruments, they also offer several other advantages:

- *Detection significance, confidence and redundancy:* a major issue with all SETI surveys historically is the significance of any claimed detection and the overall confidence in the result. This is particularly true for non-repeating signals. A radio interferometer generates multiple independent baselines, and since SETI signals are very likely to be unresolved, a signal detected in one baseline must also be detected in another. The redundancy and greater confidence made available via interferometry is an important advantage over single-dish and beam-formed instruments.
- *The invariance of position on the sky:* a general characteristic of a narrow-band SETI signal is that it is likely to drift in frequency due to the relative Doppler accelerations between the transmitter and receiver. Temporal variations in intensity might also arise due to scattering effects in the ISM or intrinsic periodicty or modulations of the transmitter. In short, for an artificial narrow-band signal, everything could be changing, with the only guaranteed invariant being the location of the transmitter on the sky (at least on short timescales- minutes to hours). Since interferometers can make images, and also locate the position of a source in the *uv* or delay-rate plane, the invariance of a SETI signal's position on the sky can be an important constraint on confirming a bona fide candidate signal. The concept is shown in Fig. 4.9.
- *Field of view:* the time and frequency resolution required by SETI observations, naturally leads to an interferometer array in which the entire field of view (only limited by the extent of the primary beam response) is available for analysis. The result is that one can descriminate between thousands of potential SETI targets in the field of view, with the prospect of studying all the targets simultaneously.
- *Sensitivity:* last but not least, it is well known that the most sensitive radio telescope arrays in the world are delivered (for unresolved sources) by VLBI. Bringing together the largest telescopes in the world into a single SETI array e.g. FAST, GBT, Arecibo, Lovell, Effelsberg, SRT, etc) would greatly improve the sensitivity provided by single dishes or small arrays.

The EVN (including *e*-MERLIN) is a facility that can have a major impact on SETI research. Although an interferometer based approach is probably not suitable for conducting large, systematic surveys of the sky (at least not yet), it can be extremely useful in (i) following-up interesting candidate signals discovered by large scale surveys (e.g. the Breakthrough Listen million star survey, Isaacson et al. 2017) and (ii) making independent observations of interesting targets (exotica) - recent examples would include the interstellar object Oumuamua, KIC 8462852 (also known as "Tabby's Star" or "Boyajian's Star") etc e.g. Enriquez et al. (2018). Observations of such exotica engage the general public in astronomical research in general, and in SETI in particular.

Some initial progress in using the EVN as a SETI search instrument has been made from the analysis of EVN archive data (ca. 2012) correlated with very fine time & frequency resolution (Garrett 2018). With only coarse data editing employed (established via obvious apriori station-based problems), RFI is essentially absent from the data at the 4σ level (see Fig. 4.9). This permitted simple limits to be placed on the presence of any artificial extraterrestrial signals in the data, with the sensitivity to a SETI signal limited by the frequency resolution of the data (32 kHz). This demonstration shows the huge potential that the EVN, *e*-MERLIN and other long-baseline arrays possess in terms of extending SETI research. With the development of the JIVE software correlator (SFXC) routinely permitting the production of correlated data with very fine frequency/time resolution, the EVN is sensitive to both narrow-band and transient signals - the characteristics one might expect from an artificial radio source. It should also be noted that in the event that an artificial signal

is detected, VLBI observations could precisely locate the position of the source (at 1 kpc, 1 AU subtends 1 mas on the sky) and reveal important details of the dynamics of the transmitter (rotation, proper motion etc.).

The detection of intelligent life outside of the Earth would be one of the most profound discoveries in the history of humankind. Such a discovery is likely to leave no aspect of human life untouched. The discovery of an independent biogenesis would provide strong evidence that intelligent life is common, and we can only guess at the ways society would be transformed if it was also possible to decode such signals. As Breakthrough Listen, and more recently NASA begin to fund the search for 'techno-signatures' at significant levels, it's important that Europe also contributes to the field. The EVN is well placed to make a real contribution to this important field.

References

Abbott, B.P. et al., 2016, *PhRvL*, **116(6)**, id.061102
Abbott, B.P. et al., 2017a, *PhRvL*, **119(16)**, id.161101
Abbott, B.P. et al., 2017b, *ApJL*, **848**, L12
Alexander, D. et al., 2016, *ApJL*, **819**, L25
Amiri, M. et al., [CHIME Collaboration], 2019, *Nature*, **566**, 230
Antoniadis, J. et al, 2015, *Science*, **340**, 1233232
Archibald, A.M., et al. 2009, *Science*, **324**, 1411
Bannister, K.W., Deller, A.T., & Phillips, C., 2019, *Science*, **365**, 565
Bassa, C. et al, 2016, *MNRAS*, **456**, 2196
Bassa, C.G. et al., 2017, *ApJ*, **843**, L8
Batejat, F. et al. *ApJ*, **740**, 95
Bietenholz, M. et al. 2014, *MNRAS*, **440**, 821
Bloom et al., 2011, *Science*, **333**, 203
Bondi, M. et al. 2012, *A&A*, **539**, A134
Brisken, W.F. et al., 2010, *ApJ*, **708**, 232
Burke-Spolaor S. et al., 2016, *ApJ*, **826**, 223
Brunthaler, A. et al. 2010, *A&A*, **516**, A27
Burrows et al., 2011, *Nature*, **476**, 421
Cameron, A.D. et al., 2018, *MNRAS*, **475**, 57
Cenko et al., 2012, *MNRAS*, **420**, 2684
Chatterjee, S. et al., 2017, *Nature*, **541**, 58
Chevalier, R., 1982, *ApJ*, **259**, 302
Chomiuk, L., 2012, *ApJ*, **750**, 164
Corbel, S. et al., 2000, *MNRAS*, **359**, 251
Cordes J.M., & Lazio T.J.W., 2003 [arXiv:astro-ph/0301598]
Corsi, A. et al. 2014, *ApJ*, **782**, 42
Corsi, A. et al., 2018, *ApJL*, **861**, L10
Coulter, D.A. et al., 2017, *GCN*, 21529
Deller, A.T. et al., 2016, *ApJ*, **828**, 8
Demorest, P.B. et al., 2010, *ApJ*, **467**, 1081
Deng, X., & Finn, L.S., 2011, *MNRAS*, **414**, 50
Eatough, R. et al. 2013, *Nature*, **501**, 391
Eftekhari, T., & Berger, E., 2017, *ApJ*, **849**, 162

Enriquez, J.E. et al., 2017, *ApJ*, **849**, 104
Enriquez, J.E. et al., 2018, *RNAAS*, **2(1)**, id. 9
Evans, C. R., & Kochanek, C. S., 1989, *ApJL*, **346**, 13
Fender, R.P., 2003, *MNRAS*, **340**, 1353
Fender, R.P., Belloni, T., & Gallo, E., 2004, *MNRAS*, **355**, 1105
Fender, R.P., Maccarone, T.J., & Heywood, I., 2013, *MNRAS*, **430**, 1538
Fialkov, A., & Loeb, A., 2017, *ApJ*, **846**, L27
Gajjar, V. et al., 2018, *ApJ*, **863**, 2
Galama, T.J. et al. 1998, *Nature*, **395**, 670
Gallo, E., et al., 2006, *MNRAS*, **370**, 1351
Gandhi, P., et al., 2019, *MNRAS*, **485**, 2642
Garrett, M.A., 2018 [arXiv:1810.07235]
Ghirlanda, G. et al., 2019, *Science*, **363**, 968 [arXiv:1808.00469]
Giacobbo, N., & Mapelli, M., 2018, *MNRAS*, **480**, 2011
Giannios, D., & Metzger, B.D., 2011, *MNRAS*, **416**, 2102
Gill, R., & Granot, J., 2018, *MNRAS*, **478**, 4128
Goldstein, A. et al., 2017, *ApJL*, **848**, L14
Granot, J., & Ramirez-Ruiz, E., 2004, *ApJL*, **609**, L9
Granot, J., & van der Horst, A.J., 2014, *PASA*, **31**, 8
Guillochon, J., & Ramirez-Ruiz, E., 2013, **ApJ**, **767**, 25
Hajela, A. et al., 2019, *ApJ*, **886**, id. L17
Hjellming, R.M., & Rupen, M.P., 1995, *Nature*, **375**, 464
Isaacson, H. et al., 2017, *PASP*, **129(975), 054501**,
Johnson, M.D., et al., 2017, *ApJ*, **850**, 172
Keimpema, A. et al., 2015, *Exp. Astr.*, **39**, 259
Kirsten, F. et al., 2014, *A&A*, **565**, A43
Komossa, S. 2015, *Journal of High Energy Astrophysics* , **7**, 148
Kramer, M., & Stappers, B., 2015, *PoS["AASKA14"]036*
Levan, D., et al., 2011, *Science*, **339**, 199
Linares, M., Shahbaz, T., & Casares, J., 2018, *ApJ*, **859**, 54
Lodato, G. et al., 2009, *MNRAS*, **392**, 332
Lorimer D.R. et al., 2007, *Science*, **318**, 777
Macquart, J.P. et al., 2015, *PoS["AASKA14"]55*
Marcaide, J.M. et al. 1995a, *Nature*, **373**, 44
Marcaide, J.M. et al. 1995b, *Science*, **270**, 1475
Marcaide, J.M. et al. 1997b, *ApJL*, **486**, 31
Marcaide, J.M. et al. 2009, *A&A*, **503**, 869
Marcote, B. et al., 2017, *ApJ*, **834**, L8
Marcote, B. et al., 2020, *Nature*, **577**, 190
Margutti, R., et al., 2018, *ApJL*, **856**, L18
Martí-Vidal, I. et al. 2011a, *A&A*, **526**, A142
Martí-Vidal, I. et al. 2011b, *A&A*, **526**, A143
Martí-Vidal, I., Pérez-Torres, M. A., & Lobanov, A.P. 2012, *A&A*, **541**, A135
Mattila, S. et al. 2018, *Science*, **351**, 62
Michilli, D. et al., 2018, *Nature*, **553**, 182
Migliari, S. et al., 2010, *ApJ*, **710**, 117

Milisavljevic, D. et al. 2015, *ApJ*, **815**, 120
Miller-Jones, J.C.A., Fender, & R.P., Nakar, E., 2006, *MNRAS*, **367**, 1432
Miller-Jones, J.C.A. et al., 2018, *MNRAS*, **479**, 4849
Miller-Jones, J.C.A. et al., 2019, *Nature*, **569**, 374
Mimica, P. et al. 2015, *MNRAS*, **450**, 2824
Mirabel, I.F., & Rodríguez, L.F., 1994, *Nature*, **371**, 46
Mirabel, I.F., & Rodríguez, L.F., 1999, *ARA&A*, **37**, 409
Modjaz, M. et al. 2016, *ApJ*, **832**, 108
Mooley, K.P. et al., 2018a, *Nature*, **554**, 207
Mooley, K.P. et al., 2018b, *Nature*, **561**, 355
Mooley, K.P. et al., 2018c, *ApJL*, **868**, L11
Mori, K., et al. 2013, *ApJ*, **770**, L23
Nakar, E., & Piran, T., 2003, *New Astronomy*, **8**, 141
Nakar, E. et al., 2018, *ApJ*, **867**, 18
Nita, G., Keimpema, A., & Paragi, Z., 2019, *Journal of Astronomical Instrumentation*, **8**, id. 1940008
Palliyaguru, N. et al., 2020, *BAAS*, **52**, id. 276.15
Papitto, A., et al., 2013, *Nature*, **501**, 517
Paragi, Z. et al., 2015, *PoS["AASKA14"]143*
Paragi, Z., 2017, *IAA RAS Transactions*, **40**, 99 [arXiv:1612.00508]
Parra, R. et al. *ApJ*, **659**, 314
Pen, U.-L. et al., 2014, *MNRAS*, **440**, 36
Pérez-Torres, M.A. et al. 2002, *MNRAS*, **335**, 23
Pérez-Torres, M.A. et al. 2005, *MNRAS*, **360**, 1055
Pérez-Torres, M.A. et al. 2014, *ApJL*, **792**, 38
Pian, E. et al., 2017, *Nature*, **551**, 67
Piran, T., 1999, *Phys. Rep.*, **314**, 575
Prochaska, J.X., Macquart, J.-P., & McQuinn, M., 2019, *Science*, **366**, 231
Ransom, S. et a., 2014, *Nature*, **505**, 520
Rampadarath, H. et al., 2012, *AJ*, **144**, 38
Ravi, A. et al., 2019, *Nature*, **572**, 352
Rees, M., 1988, *Nature*, **333**, 523
Rhoads, J. E., 1999, *ApJ*, **525**, 737
Romero-Canizales, C. et al., 2016, *ApJL*, **832**, 10
Rossi, E.M. et al., 2004, *MNRAS*, **354**, 86
Rushton, A.J., Spencer, R.E., & Strong, M. et al. 2007, *MNRAS*, **374**, L47
Rushton, A.J., et al., 2017, *MNRAS*, **468**, 2788
Salafia, O.S. et al., 2018, *A&A*, **619**, A18
Salas, P. et al. 2013, *MNRAS*, **428**, 1207
Savchenko, V. et al., 2017, *ApJL*, **848**, L15
Shannon, R.M. et al., 2018, *Nature*, **562**, 386
Siemion, A.P.V. et al., 2013, *ApJ*, **767**, 94
Soderberg, A. et al. 2005, *ApJ*, **621**, 908
Spencer, R.E., et al., 2013, *MNRAS*, **435**, L48
Spitler L.G. et al., 2016, *Nature*, **531**, 202
Stinebring, et al., 2001, *ApJ*, **549**, 97
Stovall, K., et al. 2018, *ApJ*, **854**, 22